Bioorganic & Medicinal Chemistry Letters 20 (2010) 4800–4804

Contents lists available at ScienceDirect

Bioorganic & Medicinal Chemistry Letters

journal homepage: www.elsevier.com/locate/bmcl

Discovery and optimization of pyrazoline compounds as B-Raf inhibitors

Matthew O. Duffey *, Ruth Adams, Christopher Blackburn, Ryan W. Chau, Susan Chen, Katherine M. Galvin, Khristofer Garcia, Alexandra E. Gould, Paul D. Greenspan, Sean Harrison, Shih-Chung Huang, Mi-Sook Kim, Bheemashankar Kulkarni, Steven Langston, Jane X. Liu, Li-Ting Ma, Saurabh Menon, Masayuki Nagayoshi, R. Scott Rowland, Tricia J. Vos, Tianlin Xu, Johnny J. Yang, Shaoxia Yu, Qin Zhang

Millennium Pharmaceuticals, Inc., Oncology, Medicinal Chemistry, 40 Landsdowne St., Cambridge, MA 02139, United States

ARTICLE INFO

Article history:
Received 11 May 2010
Revised 17 June 2010
Accepted 21 June 2010
Available online 25 June 2010

Keywords:
B-Raf
B-Raf inhibitor
Pyrazoline

ABSTRACT

The discovery of novel pyrazoline derivatives as B-Raf (V600E) inhibitors is described in this report. Chemical modification of the pyrazoline scaffold led to the development of SAR and identified potent and selective inhibitors of B-Raf (V600E). Determination of the pharmacokinetic properties of selected inhibitors is also reported.

Raf, a serine/threonine protein kinase, is an integral part of the MAP kinase signaling pathway and is involved in the Ras signaling cascade of Raf-MEK-ERK.[1] Uncovering the complex and intricate role of Raf pathway signaling in cancer is the continuing aim of intensive research.[2] Activating mutations of the Raf isoform B-Raf cause constitutive activation of the MAP kinase pathway and uncontrolled proliferation of tumor cells. Specific mutations of B-Raf are associated with various cancers including non-Hodgkin's lymphoma, colorectal adenocarcinoma, malignant melanoma, thyroid carcinoma, non-small cell lung carcinoma, and adenocarcinoma of the lung. Studies report that B-Raf mutations exist in up to 66% of malignant melanomas with a single mutation (V600E) accounting for 80% of these.[3] Suppression of B-Raf (V600E) in human melanoma cells leads to downregulation of the MAP kinase signaling pathway and apoptosis.[4] Recently, treatment of B-Raf mutant melanoma patients with a selective B-Raf inhibitor (PLX-4032) resulted in promising preliminary evidence of antitumor activity.[5] Thus, inhibition of mutated B-Raf could prove to be a useful therapeutic against melanoma as well as a number of other cancers.

An inhibitor (**1**) of B-Raf (V600E) was initially identified by high-throughput screening of our compound library (Fig. 1). We became interested in this initial hit due to the novelty of the pyrazoline scaffold as well as its biological activity. In vitro enzyme and cell assays were employed to evaluate compound activity against the target.[6]

Optimization of **1**, with respect to enzyme and cellular potency, began with the synthesis of numerous analogues by parallel synthesis (Fig. 1). The rapid synthesis of analogues via acylation of the parent pyrazoline provided an opportunity for the screening of a diverse set of compounds possessing replacements of the furan moiety. We felt this was a natural starting point for analogue synthesis as the furanoyl moiety could easily be replaced by a diverse array of acylating agents. Implementation of this strategy led to the identification of thiophene–pyridine as a furan replacement to give **2**, a compound that showed a significant potency increase in the in vitro assays.[7]

To better understand the activity of **2**, an analysis of its binding to B-Raf was performed (Fig. 2). Represented by white carbons, **2**

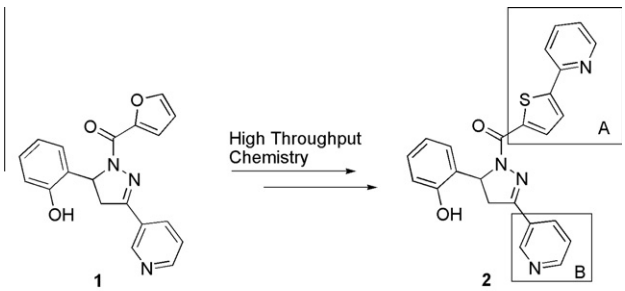

Figure 1. Initial HTS hit and high-throughput chemistry optimization of **1**.

* Corresponding author. Tel.: +1 617 551 7832; fax: +1 617 551 8907.
E-mail address: matthew.duffey@mpi.com (M.O. Duffey).

0960-894X/$ - see front matter © 2010 Elsevier Ltd. All rights reserved.
doi:10.1016/j.bmcl.2010.06.113

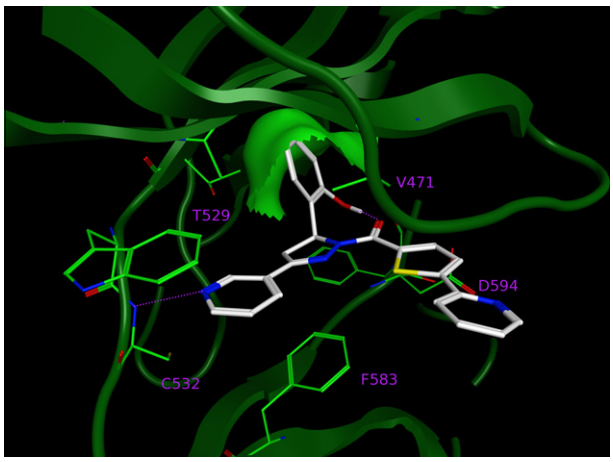

Figure 2. Proposed binding mode of **2**.

was docked into a homology model of wild type B-Raf based on a crystal structure of B-Raf bound sorafenib (PDB 1UWH)[8] but modified to an active kinase conformation (DFG-in).[9] In this model, the nitrogen of the pyridine ring (region B) forms a hydrogen bond to the hinge backbone NH of C532. In the back of the ATP pocket an intramolecular hydrogen bond between the hydrogen of the phenolic OH and the carbonyl of the pyrazoline amide helps organize the phenol in a hydrophobic pocket (green surface). In addition, the thiophene–pyridine extends under the P loop out towards solvent.

At this point we focused our efforts on a traditional medicinal chemistry approach to optimize **2**. Our goals were foremost to improve potency and understand the SAR of B-Raf (V600E) inhibition. The strategy devised to accomplish this task involved modification of the three substituents of the central pyrazoline core. Initial chemistry efforts that led to discovery of **2** from **1** demonstrated that replacement of the furan ring with a biaryl system increased potency.[7] We wished to expand upon this discovery and evaluate compounds that explored this area of the scaffold further (region

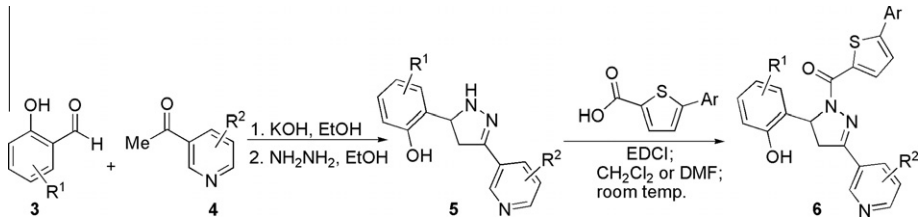

Scheme 1. Synthetic scheme to construct substituted pyrazolines.

Table 1
SAR/optimization of region A

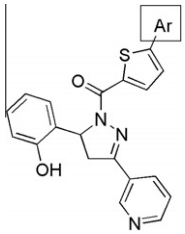

	Ar	V600E IC_{50}[a] (nM)	pERK IC_{50}[a] (nM)		Ar	V600E IC_{50}[a] (nM)	pERK IC_{50}[a] (nM)
2		23 ± 7	180 ± 40	**12**	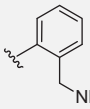	10 ± 6	270 ± 77
7		79	1500	**13**	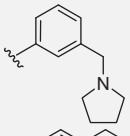	6	110 ± 54
8	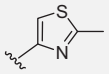	7 ± 4	210	**14**	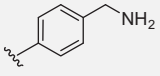	5 ± 1	82 ± 38
9	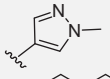	9	89 ± 48	**15**	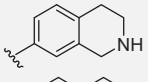	4	25 ± 9
10	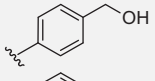	5	140 ± 120	**16**	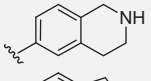	5	21 ± 9
11	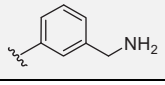	6 ± 1	390 ± 200	**17**	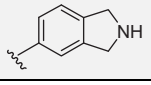	4	19 ± 1

[a] Standard deviations are reported for $N \geqslant 3$. Otherwise IC_{50} values are mean values of two determinations.

Table 2
SAR/optimization of phenol

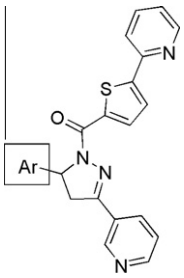

	Ar	V600E IC_{50}[a] (nM)	pERK IC_{50}[a] (nM)		Ar	V600E IC_{50}[a] (nM)	pERK IC_{50}[a] (nM)
18		799	nd	**21**	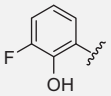	13	1400
19	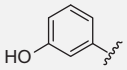	670 ± 320	>25,000	**22**	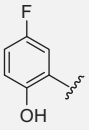	7	680
20	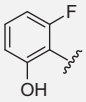	5 ± 1	80 ± 29	**23**	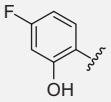	11	1400

[a] Standard deviations are reported for $N \geqslant 3$. Otherwise IC_{50} values are mean values of two determinations.

A). In addition, modification of the pyridine ring (region B) and the phenol were also investigated.

Scheme 1 shows the general route employed to synthesize the desired pyrazoline analogues. The core pyrazoline functionality (**5**) was made via a two-step process in which aldol condensation between an appropriately substituted acetylpyridine (**3**) and a 2-hydroxybenzaldehyde (**4**)[10] was followed by pyrazoline formation by addition of hydrazine.[11] A standard amide coupling between **5** and an appropriate thiophene carboxylic acid then completed the synthesis to provide general structure **6**.[12]

Use of the route in Scheme 1 allowed for the construction of numerous analogues that initially explored the effect of the outer aryl ring of region A. While the discovery of **2** demonstrated that an aromatic ring is beneficial at this site, further chemical manipulation of this site confirmed this finding. In doing so, we made an effort to choose aryl rings that contained solubilizing groups as the aqueous solubility of **2** was so low (5.8 μg/mL)[13] we were unable to formulate IV doses for pharmacokinetic experiments.

Table 1 shows the results of these efforts. Replacement of the 2-pyridyl ring with an *o*-tolyl ring resulted in loss of activity (**7**) while other heterocycles such as thiazole and pyrazole maintained enzyme and cell potency (**8**, **9**). *p*-Benzyl alcohol provided a compound (**10**) with good enzyme and cell potency, as did the installation of benzyl amines (**11**–**14**). Significant increases in cell potency were observed upon use of constrained amines such as the isomeric tetrahydroisoquinoline moieties (**15**, **16**) and the isoindoline functionality (**17**). We were unable to identify a reason for the discrepancy between the enzyme and cell assays (permeability/solubility were not the cause). As a result, our evaluation of potency relied largely on the results of the cell assay as it gave us the ability to distinguish between compounds that possessed good potency in the enzyme assay.

Analogues were also prepared to explore SAR of the phenol ring (Table 2). Removal of the OH (**18**) or placement of the OH in the *meta* position (**19**) resulted in a loss of enzyme and cell activity, suggesting that the intramolecular H-bonding of the C1–OH as proposed by our homology model is essential for potency. With this insight, we focused our efforts on substitution of the phenol to

Table 3
ortho-Fluoride enhances potency

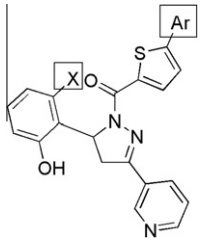

	Ar	X	V600E IC_{50}[a] (nM)	pERK IC_{50}[a] (nM)
20		F	5 ± 1	80 ± 29
2		H	23 ± 7	180 ± 40
24	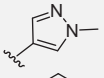	F	3	55 ± 19
9		H	9	89 ± 48
25	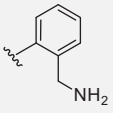	F	7 ± 6	85 ± 38
12		H	10 ± 6	200 ± 77
26	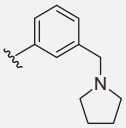	F	8	41 ± 9
13		H	6	110 ± 54
27	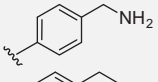	F	3	37 ± 10
14		H	5 ± 1	82 ± 38
28	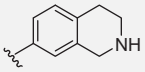	F	3	21 ± 10
15		H	4	25 ± 9
29	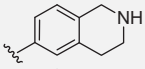	F	3	34 ± 11
16		H	5	21 ± 9
30	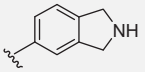	F	2	60
17		H	4	19 ± 1

[a] Standard deviations are reported for $N \geqslant 3$. Otherwise IC_{50} values are mean values of two determinations.

Table 4
SAR/optimization of region B

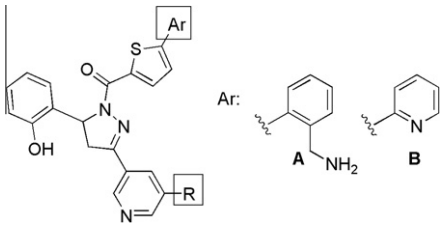

	Ar	R	V600E IC_{50}[a] (nM)	pERK IC_{50}[a] (nM)		Ar	R	V600E IC_{50}[a] (nM)	pERK IC_{50}[a] (nM)
12	A	H	10 ± 6	200 ± 77	**2**	B	H	23 ± 7	180 ± 40
31	A	F	21 ± 17	180 ± 67	**33**	B	NHAc	3 ± 0.2	63 ± 27
32	A	NH_2	7	64 ± 36	**34**	B	CH_2OH	3	39 ± 22
					35	B	NH_2	3	31 ± 6

[a] Standard deviations are reported for $N \geqslant 3$. Otherwise IC_{50} values are mean values of two determinations.

Table 5
Optimization of the three regions

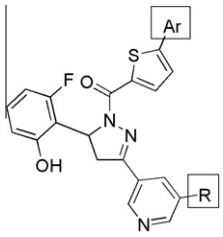

	Ar	R	V600E IC_{50}[a] (nM)	pERK IC_{50}[a] (nM)
36	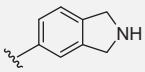	CH_2OH	3	120
37	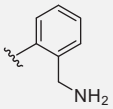	NH_2	4	56
38		NH_2	3	18 ± 8

[a] Standard deviations are reported for $N \geqslant 3$. Otherwise IC_{50} values are mean values of two determinations.

Table 6
Pharmacokinetic data for B-Raf (V600E) inhibitors[15]

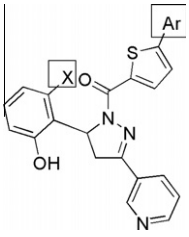

	Ar	X	pERK IC_{50}[a] (nM)	CL (L/h/kg)	AUC (nM h)	%*F*
17	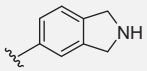	H	19 ± 1	3.5	890	14
30		F	60	0.9	8400	37
12	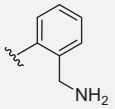	H	200 ± 77	3.9	4900	76
25		F	85 ± 38	1.6	11,000	85
39	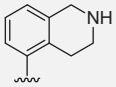	F	180	0.7	26,000	89

[a] Standard deviations are reported for $N \geqslant 3$. Otherwise IC_{50} values are mean values of two determinations.

determine the effect of further changes. We found that incorporation of fluoride in the ring (C-1) resulted in increased potency (**20**). In turn, the subsequent transfer of the fluoride to other positions on the ring resulted in varying degrees of decreased cell potency (**21**–**23**).

Fluoride incorporation at C-1 of the phenol ring provided compounds that generally were more potent than their non-fluorinated counterparts in the cell assay. Table 3 shows the comparison between selected compounds with and without the C-1 fluoride on the phenol. In general, a 2–3-fold increase in cell potency was observed for the fluorinated analogues. While nitrogen-containing heterocycles gave potent analogues (**20**, **24**) so did benzylamines substituted at the *ortho*, *meta*, and *para* positions (**25**–**27**). Ultimately, the most potent compounds in the cell assay remained the isomeric tetrahydroisoquinoline analogues (**28**, **29**) while the isoindoline decreased in potency with the addition of fluoride (**30**). We also obtained selectivity data for **26**. In a broad multikinase binding screen, only 8 of 359 kinases screened were inhibited greater than 50% in the presence of 1 μM of **26**.[14]

We also explored the effect changes in region B had upon activity (Table 4). While we learned that the 3-pyridyl ring was critical for potency against the target (data not shown), we also observed that substitution at C-5 of the pyridyl ring could provide a boost in cell potency. We created analogues in two subseries, one containing the *ortho* benzylamine and the other containing the 2-pyridyl group in region A as shown in Table 4. Addition of fluoride (**31**) provided an analogue that was equipotent with **2**, while addition of the amino (**32**, **35**), acylamino (**33**) and hydroxymethyl (**34**) groups to this ring gave a significant increase in cell potency.

We attempted to combine the optimal modifications of these three regions by using the same synthetic techniques described previously. Representative compounds are shown in Table 5. By inclusion of the C-1 fluorophenol and varying the outer aryl ring of region A, we learned that the positive trends in cell potency are additive in some cases while not in others. Combination of the hydroxymethyl moiety in ring B with the bicyclic amine did not provide an increase in cell potency (**36**). However, combining the 3-aminopyridine in region B with the benzyl amine or pyridine in region A provided very potent compounds in the cell assay, including one of the most potent compound synthesized in this study of B-Raf inhibitors (**38**).

As significant potency gains had been made in the chemical series, an evaluation of the pharmacokinetic properties of the series became a priority (Table 6). While insolubility of **2** prevented us from formulating it for IV dosing, we were pleased to find that modification of the scaffold improved solubility sufficiently to allow most compounds to be formulated for IV dosing. When dosing in rats (IV and PO)[15] in general, non-fluorinated analogues suffered from high clearance or low bioavailability, or both. This, in turn, led to low plasma exposures (**17**, **12**). Fortuitously, the addition of fluoride to the phenol ring led to compounds that possess higher bioavailability and lower rates of clearance from plasma than their non-fluorinated counterparts. This resulted in a marked increase in plasma exposures (**30**, **25**). In particular, the tetrahydroisoquinoline analogue should be highlighted (**39**). It is an example of a fluorinated analogue that possesses low clearance and high bioavailability resulting in the highest plasma exposure levels we observed in this study. In contrast, region B analogues all showed poor pk properties, with or without incorporation of the C-1 fluorophenol (data not shown).

We have discovered a series of novel inhibitors of mutant B-Raf (V600E). The modular structure of the pyrazoline scaffold lent itself well to analogue synthesis and we synthesized compounds that are very potent in vitro. In particular, the discovery of the addition of the C-1 fluoride to the phenol provided a significant increase in cell potency. Furthermore, we have also identified fluorinated compounds that possess outstanding pharmacokinetic properties and in depth examination of these compounds in vivo activities is warranted.

References and notes

1. Robinson, M. J.; Cobb, M. H. *Curr. Opin. Cell Biol.* **1997**, *9*, 180.
2. (a) Heidorn, S. J.; Milagre, C.; Whittaker, S.; Nourry, A.; Niculesu-Davas, I.; Dhomen, N.; Hussain, J.; Reis-Filho, J. S.; Springer, C. J.; Pritchard, C.; Marais, R. *Cell* **2010**, *140*, 209; (b) Poulikakos, P. I.; Zhang, C.; Bollag, G.; Shokat, K. M.; Rosen, N. *Nature* **2010**, *464*, 427; (c) Hatzivassiliou, G.; Song, K.; Yen, I.; Brandhuber, B. J.; Anderson, D. J.; Alvarado, R.; Ludlam, M. J. C.; Stokoe, D.; Gloor, S. L.; Vigers, G.; Morales, T.; Aliagas, I.; Liu, B.; Sideris, S.; Hoeflich, K. P.; Jaiswal, B. S.; Seshagiri, S.; Koeppen, H.; Belvin, M.; Friedman, L. S.; Malek, S. *Nature* **2010**, *464*, 431.
3. Davies, H.; Bignell, G. R.; Cox, C.; Stephens, P.; Edkins, S.; Clegg, S.; Teague, J.; Woffendin, H.; Garnett, M. J.; Bottomley, W.; Davis, N.; Dicks, E.; Ewing, R.; Floyd, Y.; Gray, K.; Hall, S.; Hawes, R.; Hughes, J.; Kosmidou, V.; Menzies, A.; Mould, C.; Parker, A.; Stevens, C.; Watt, S.; Hooper, S.; Wilson, R.; Jayatilake, H.; Busterson, B. A.; Cooper, C.; Shipley, J.; Hargrave, D.; Pritchard-Jones, K.; Maitland, N.; Chenevix-Trench, G.; Riggins, G. J.; Bigner, D. D.; Palmieri, G.; Cossu, A.; Flanagan, A.; Nicholson, A.; Ho, J. W. C.; Leung, S. Y.; Yuen, S. T.; Weber, B. L.; Seigler, H. F.; Darrow, T. L.; Paterson, H.; Marais, R.; Marshall, C. J.; Wooster, R.; Stratton, M. R.; Futreal, P. A. *Nature* **2002**, *417*, 949.
4. Hingorani, S. R.; Jacobetz, M. A.; Robertson, G. P.; Herlyn, M.; Tuveson, D. A. *Cancer Res.* **2003**, *63*, 5198.
5. Flaherty, K.; Puzanov, I.; Sosman, J.; Kim, K.; Ribas, A.; McArthur, G.; Lee, R. J.; Grippo, J. F.; Nolop, K.; Chapman, P. *J. Clin. Oncol.* **2009**, *27*, 15s.
6. (a) Raf activity was determined using a 384 well streptavidin coated flashplate. Reactions were performed with biotinylated peptide substrate at 30 °C for 3 h in a final volume of 30 μL. After addition of stop the reaction was incubated on a flashplate for 2 h. The flashplates were read on a Topcount counter.; (b) The whole cell ELISA assay utilized a human melanoma cell line (A375) possessing the mutation BRaf V600E. A375 cells seeded overnight were incubated with Raf inhibitors for 3 h. At the end of the incubation, the cells were fixed, permeabilized, blocking buffer added and the plates were incubated overnight. After the blocking buffer was discarded, the plates were incubated with anti-phospho-ERK antibody for 1 h followed by treatment with anti-horse radish peroxidase. Optical density was read at 650 nm for tetramethylbenzidine as substrate.
7. Blackburn, C.; Duffey, M. O.; Gould, A. E.; Kulkarni, B.; Liu, J. X.; Menon, S.; Nagayoshi, M.; Vos, T. J.; Williams, J. *Bioorg. Med. Chem. Lett.* **2010**, *20*, 4795.
8. Wan, P. T. C.; Garnett, M. J.; Roe, S. M.; Lee, S.; Niculescu-Duvaz, D.; Good, V. M.Cancer Genome Project, Jones, C. M.; Marshall, C. J.; Springer, C. J.; Barford, D.; Marais, R. *Cell* **2004**, *116*, 855.
9. We initially used a homology model because no DFG-in structures were available. When these structures became available, they were found to be nearly identical to the homology model. Initial attempts to dock **2** in the DFG-out conformation proved to be unsatisfactory.
10. Annigeri, A. C.; Siddappa, S. *Indian J. Chem.* **1963**, *1*, 484.
11. Lange, J.; Coolen, H.; van Stuivenberg, H.; Dijksman, J.; Herremans, A.; Ronken, E.; Keizer, H.; Tipker, K.; McCreary, A.; Veerman, W.; Wals, H.; Stork, B.; Verveer, P.; den Hartog, A.; de Jong, N.; Adolfs, T.; Hoogendoorn, J.; Kruse, C. *J. Med. Chem.* **2004**, *47*, 627.
12. Compounds were synthesized as racemic mixtures. The enantiomers of **2** were separated via chiral HPLC revealing one enantiomer to be active (pERK IC_{50}: 280 nM) and the other to be inactive (pERK IC_{50}: 14 μM). Due to ease of synthesis and time consuming methods required for HPLC separation we evaluated all compounds as racemic mixtures.
13. Solubility was determined by a turbidimetric solubility assay which provides the kinetic solubility of compounds in 50 mM potassium phosphate buffer at pH 6.8.
14. Developed and marketed by Ambit Biosciences, KINOME*scan*™ is a competition binding assay that quantitatively measures the ability of a compound to compete with an immobilized, active-site directed ligand (see: http://www.kinomescan.com). Kinases inhibited >50% included DDR1(54%), DDR2(60%), EGFR(L747-S752$_{del}$ P753S)(58%), EGFR(S752-I759$_{del}$)(55%), EPHB3(65%), KIT(D816 V)(95%), LCK(66%), and RET(M918T)(70%). B-Raf (V600E) and WT B-Raf were both inhibited at 100%. IC_{50} data was not generated in the Ambit assay. In-house enzyme assays revealed the related compound **2** to be equipotent against B-Raf (V600E) (IC_{50}: 23 nM), WT B-Raf (IC_{50}: 17 nM), and C-Raf (IC_{50}: 27 nM).
15. Pharmacokinetic experiments were performed by dosing either intravenously (0.5 mg/kg or 1 mg/kg) or orally (10 mg/kg) in male SD rats.